Tribology Letters (2026) 74:49
https://doi.org/10.1007/s11249-026-02134-z

ORIGINAL PAPER

An extended Griffith friction model for the transition to slip in the contact of graded-material spheres

Shi-Wen Chen[1] · Gang-Feng Wang[1] · Michele Ciavarella[2,3]

Received: 8 December 2025 / Accepted: 17 March 2026

Abstract
In the present paper, we study the role of gradient in the material properties of contacting bodies in the difference between static and kinetic friction for a Hertzian geometry, according to the theory of "Griffith friction", for which the transition from stick to slip occurs as an elastic instability. We use the term "Griffith friction" to suggest an energy balance approach in mode II to derive stable and unstable equilibrium configurations, where in particular macroscopic sliding can occur by a global elastic instability, analogous to a Griffith crack which doesn't arrest after reaching a critical size. The most important conclusion are that static friction coefficient: (i) is increased with harder surface; (ii) is increased for small normal loads and tends to infinity in the limit of zero load. These conclusions hold both in the case of a constant frictional fracture energy or a pressure-dependent frictional fracture energy at the interface.

Keywords Graded material · Griffith friction · Cattaneo-Mindlin problem · Friction

1 Introduction

Friction is always present at interacting interfaces in relative motion, with applications spanning from science to engineering to geophysics, namely from the atomic (nano) scale to earthquake faults in the range of thousands of kilometers. In the classical view of friction, as proposed by Amontons and Coulomb the friction force is proportional to the normal load, and there is no significant distinction between static and dynamic (or kinetic) friction coefficient, as was instead proposed by Euler through experiments using inclined planes. Rabinowicz [1, 2] was the first to associate and demonstrate via careful experiments that the reduction of friction in the transition from stick to sliding is due to the interfacial energy of metals. In the mechanics of earthquake faults the difference between static and kinetic coefficient has been reported to be as high as 10, which is why Rice calls such interfaces "strong but brittle"[3, 4]. After concepts of fracture mechanics were introduced into contact mechanics for adhesion and friction in the 1970's [5–9], it became obvious that both the detachment in the normal direction ("pull-off"), and the detachment in the tangential direction (transition to slip) can be mechanisms associated to elastic instabilities. Additionally, the JKR-type peeling and sliding models, developed in recent years to describe the interplay between adhesion and friction, have also been applied to analyze experimental data [10].

Recently, Ciavarella [11] has introduced the solution to the Cattaneo-Mindlin problem [12, 13] with Griffith friction, where a constant normal load is considered at the interface, and tangential load is progressively increased until a peak tangential force is reached leading to an unstable transition to slip at lower friction. This was proved to be a reasonable model also to fit experiments of Peng et al. [14], see Ref. [15].

In the present paper, we aim at elucidating the role of gradient in the material properties of contacting bodies in the difference between static and kinetic friction. Gradient in material properties exists both in Nature or are intentionally introduced by technological processes because they lead to for example some improvements of thermomechanical properties of components. Indeed, Functionally Graded Materials (FGM) can be seen as a generalization of using layered

✉ Michele Ciavarella
Mciava@poliba.it

[1] Department of Engineering Mechanics, SVL and MMML, Xi'an Jiaotong University, Xi'an 710049, People's Republic of China

[2] DMMM department, Politecnico di Bari, Viale Gentile 182, Bari 70126, Italy

[3] Department of Mechanical Engineering, Hamburg University of Technology, Am Schwarzenberg-Campus 1, Hamburg 21073, Germany

Published online: 29 April 2026

structures as coatings, plating techniques or layer lamination process [16–18]. FGM became increasingly popular since 1990 s. The idea is to gradually vary the composition and structure of the material so that this results in a continuous variation of properties of materials, particularly the elastic properties, removing some of typical problems of layered materials as poor interface strength and residual stresses. But returning to Nature, living species and evolution has "invented" FGM millions of years ago, and indeed graded media are found in many biological structures as bones, skin or bamboo trees [19]. Significant work has been produced both for the development of the manufacturing techniques of FGM and on the other hand for studying their behavior and structural integrity [20–22]. Another important area where FGM are studied is soil mechanics and geomechanics where the graduality of properties occurs naturally as a consequence of the change of rocks content. This has an effect in engineering too, as the variation of elastic properties of soils and rocks may affect the settlement and stability of foundations [23–25].

In many cases the spatial variation of elastic modulus with depth is assumed to follow either an exponential or a power law, although the latter leads to rather extreme assumption of either zero or infinite modulus at the surface [22]. Analytical solutions for some types of surface loading can be obtained within this class of FGM, see Booker et al. [26, 27], and Giannakopoulos and Suresh [28, 29].

It is interesting to notice also that Giannakopoulos and Suresh [30, 31] also demonstrated with theory and experiments that grading material properties under both normal and frictional indentation is beneficial against various types of brittle failures due to contact.

2 Methodology

In this study, we consider two elastic spheres brought into contact under a fixed normal load P and subsequently subjected to a tangential load Q, as illustrated in Fig. 1. Since the radii of the spheres are much larger than the contact radius, both elastic spheres can be approximated as elastic half-spaces. The materials of the two deformable bodies are functionally graded, and their elastic modulus varies with depth according to

$$E_i(z) = E_{0i}\left(\frac{z}{z_0}\right)^k, \text{ with } -1 < k \leqslant 1, \ i = 1, 2. \tag{1}$$

We assume that the two materials have the same grading exponent k and characteristic length z_0. The Poisson's ratios are denoted by ν_1 and ν_2, respectively. Similar to the original Cattaneo-Mindlin model, the normal and tangential contact

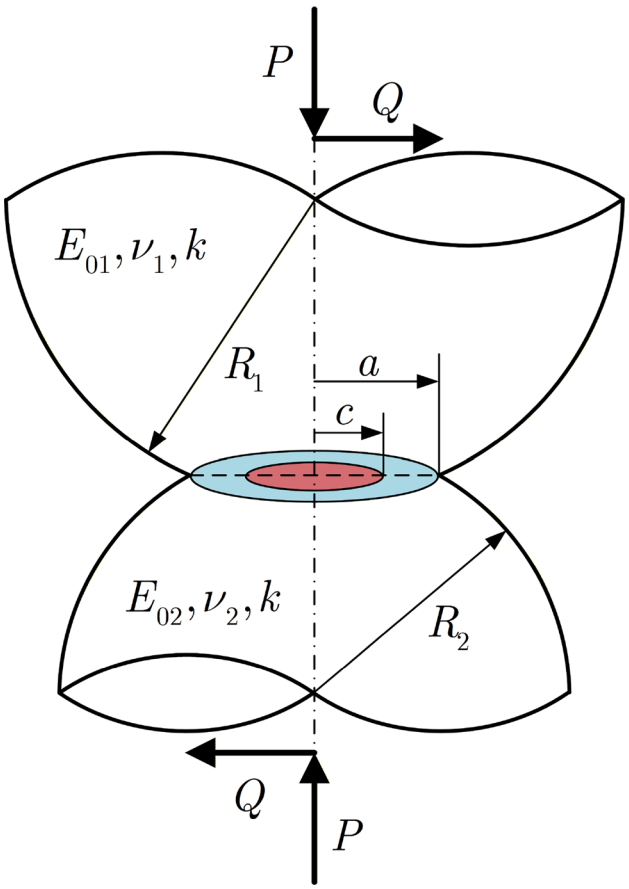

Fig. 1 Schematic illustration of the contact between two spheres under a normal load P and a tangential load Q

problems are assumed to be decoupled. This decoupling requires either that [32]:

1. Equal elastic materials: $\nu_1 = \nu_2 = \nu$ and $E_{01} = E_{02}$;
2. One body is rigid and the other elastic with a Poisson's ratio equal to the Holl ratio: $E_{0i} \to \infty$ and $\nu_j = 1/(2+k)$ with $i \neq j$;
3. The Poisson's ratios of both materials are given by the Holl ratio: $\nu_1 = \nu_2 = 1/(2+k)$.

Moreover, it is noteworthy that due to thermodynamic stability, the Holl ratio can only be fulfilled for positive k.

On the other hand, in the classical homogeneous Cattaneo-Mindlin model, the tangential-tangential coupling is often regarded as a minor error issue and is therefore commonly neglected. However, for functionally graded materials, the influence of tangential-tangential coupling may become much more significant. As discussed by Hess and Li [37], even in the case of equal elastic materials, tangential-tangential decoupling can only be achieved for specific combinations of the material parameters (k, ν). In the following analysis, in order to present the main idea of the proposed

model more clearly, we do not strictly enforce these specific (k, ν) conditions. The effect of tangential-tangential coupling, particularly under general parameter combinations, may therefore deserve a more rigorous and systematic investigation in future work.

It is worth noting that, under small deformation conditions, the contact and friction problem between two spheres can be equivalently reduced to the contact between a sphere of radius R and an elastic half-space, where the effective radius satisfies

$$\frac{1}{R} = \frac{1}{R_1} + \frac{1}{R_2}. \tag{2}$$

2.1 Uniform normal and tangential displacement solutions

The solutions for contact problems with axisymmetric contact areas can be obtained by superposing elementary solutions corresponding to a constant surface displacement over a circular region [33–35]. In the normal direction, if the displacement within a circular region of radius a is uniform and equal to d_z, the total normal force P_0 and the corresponding pressure distribution $p_0(r, a)$ are given by Booker et al. as [27]

$$P_0 = \frac{2E_0^* a^{1+k}}{(1+k)\, z_0^k} d_z, \tag{3}$$

$$p_0(r, a) = \frac{(1+k)\, P}{2\pi a^2} \left(1 - \frac{r^2}{a^2}\right)^{\frac{k-1}{2}}, \tag{4}$$

where $E_0^*(k, \nu_i, E_{0i})$ is determined by

$$\frac{1}{E_0^*} = \frac{1-\nu_1^2}{h_N(k, \nu_1)\, E_{01}} + \frac{1-\nu_2^2}{h_N(k, \nu_2)\, E_{02}}, \tag{5}$$

and the function $h_N(k, \nu)$ is originally defined in Ref.[36] as

$$h_N(k, \nu) = \frac{2(1+k)\cos\left(\frac{k\pi}{2}\right)\Gamma\left(1+\frac{k}{2}\right)}{\sqrt{\pi}\, C(k, \nu)\, \beta(k, \nu) \sin\left(\frac{\beta(k,\nu)\pi}{2}\right)\Gamma\left(\frac{1+k}{2}\right)}, \tag{6}$$

with

$$C(k, \nu) = \frac{2^{1+k}\Gamma\left(\frac{3+k+\beta(k,\nu)}{2}\right)\Gamma\left(\frac{3+k-\beta(k,\nu)}{2}\right)}{\pi\Gamma(2+k)}, \tag{7}$$

and

$$\beta(k, \nu) = \sqrt{(1+k)\left(1 - \frac{k\nu}{1-\nu}\right)}. \tag{8}$$

Here, $\Gamma(\cdot)$ denotes the Gamma function, defined by

$$\Gamma(z) = \int_0^\infty t^{z-1} \exp(-t)\, \mathrm{d}t. \tag{9}$$

The solution for a uniform tangential displacement d_x imposed over a circular region of radius a has also been developed in previous work by Hess et al. [36, 37]. The total tangential force Q_0 and the corresponding distribution of the unidirectional tangential traction $q_0(r, a)$ are given by

$$Q_0 = \frac{2G_0^* a^{1+k}}{(1+k)\, z_0^k} d_x, \tag{10}$$

$$q_0(r, a) = \frac{(1+k)\, Q}{2\pi a^2} \left(1 - \frac{r^2}{a^2}\right)^{\frac{k-1}{2}}, \tag{11}$$

where $G_0^*(k, \nu_i, E_{0i})$ is determined by

$$\frac{1}{G_0^*} = \frac{1}{h_T(k, \nu_1)\, E_{01}} + \frac{1}{h_T(k, \nu_2)\, E_{02}}, \tag{12}$$

and the function $h_T(k, \nu)$ is also originally defined in Ref.[36] as

$$h_T(k, \nu) = \frac{2\beta(k, \nu)\cos\left(\frac{k\pi}{2}\right)\Gamma\left(1+\frac{k}{2}\right)}{(1-\nu^2)\sqrt{\pi}\, C(k, \nu)\sin\left(\frac{\beta(k,\nu)\pi}{2}\right)\Gamma\left(\frac{3+k}{2}\right) + \beta(k, \nu)(1+\nu)\Gamma\left(1+\frac{k}{2}\right)}. \tag{13}$$

By comparing the solutions in the normal direction, Eqs. (3) and (4), with those in the tangential direction, Eqs. (10) and (11), and noting that the uniform-displacement solutions serve as the basis for any axisymmetric contact solution, one finds that for the same axisymmetric displacement distribution or the same force distribution, the corresponding tangential solution can be obtained from the normal one by replacing $E_0^*(k, \nu_i, E_{0i})$ with $G_0^*(k, \nu_i, E_{0i})$.

2.2 Cattaneo-Mindlin problem

In the Cattaneo-Mindlin (CM) problem [12, 13], it is assumed that the contact area consists of a central stick zone, where the relative surface displacement is zero, and an outer slip zone, where the tangential traction and the normal pressure satisfy Coulomb's friction law. Over the past century, the Cattaneo-Mindlin friction model has been generalized to a wide range of cases, including elastically similar, transversely isotropic solids of arbitrary geometry [38]. Under the assumption of normal-tangential decoupling, and neglecting the displacement components in the slip zone that are not aligned with the direction of the tangential force Q, as is customary in the

Cattaneo-Mindlin solution and in the Ciavarella-Jager theorem, the distribution of the tangential traction within the contact area can be written as

$$q(r) = fp(r,a) - q^*(r,c), \ r < c, \tag{14}$$
$$q(r) = fp(r,a), \ c \leqslant r < a. \tag{15}$$

where c denotes the radius of the stick zone, f denotes the kinetic friction coefficient, and $q^*(r,c)$ is a corrective term that ensures the relative displacement within the stick zone remains constant, representing a rigid-body displacement. Here, $p(r,a)$ denotes the normal pressure in the spherical normal contact problem. For a graded material characterized by Eq. (1), it is given by [32]

$$p(r,a) = \frac{(3+k)\,P_1(a)}{2\pi a^2}\left(1-\frac{r^2}{a^2}\right)^{\frac{1+k}{2}}, \tag{16}$$

where

$$P_1(a) = \frac{4E_0^* a^{3+k}}{z_0^k (1+k)^2 (3+k) R}, \tag{17}$$

and the corresponding normal relative rigid-body displacement δ_z is given by

$$\delta_z = \frac{a^2}{(1+k)R} \tag{18}$$

In the classical CM model, the corrective term is taken as $fp(r,c)$, which produces the same profile of tangential displacement as $fp(r,a)$ and therefore ensures that the relative displacement vanishes within the region of radius c.

2.3 Griffith friction

In the classical CM model, slip is assumed to occur immediately once the tangential traction reaches the kinetic friction level. Experiments, however, have shown that the onset of slip requires overcoming an energy barrier [39]. To capture a more realistic transition from static to kinetic friction, a Griffith/JKR-type slip-initiation criterion can be incorporated into the CM framework, leading to the development of the Griffith friction model [11].

The Griffith friction framework is analogous to the classical CM model, but the corrective term is derived from fracture mechanics. This term reflects interfacial fracture processes, primarily mode II, along with contributions from mode III [40]. In general, we would need averaging the stress intensity factor K_{II} and K_{III} around the periphery of the contact. However, by neglecting Poisson effects, the energy release rate can be approximated as purely mode II. The formulation of the corrective term is analogous to that of the Johnson-Kendall-Roberts (JKR) adhesion model [5], ensuring that the relative displacement remains zero within the stick zone. The key distinction is that the corrective term of Griffith friction involves shear tractions rather than normal pressures.

The corrective term for Griffith friction, denoted as q^*_{JKR}, can be decomposed into two parts: one that generates a spherical tangential displacement profile, and another that produces a constant displacement. It can be written as

$$q^*_{\mathrm{JKR}}(r,c) = \frac{(3+k)\,Q_1(c)}{2\pi c^2}\left(1-\frac{r^2}{c^2}\right)^{\frac{k+1}{2}} - \frac{(1+k)\,Q_2(c)}{2\pi c^2}\left(1-\frac{r^2}{c^2}\right)^{\frac{k-1}{2}}, \tag{19}$$

where $Q_1(c)$ is equal to $fP_1(c)$. If the frictional fracture energy is denoted by γ, which is defined in analogy to the work of adhesion but accounting for the contributions of mode II and mode III interfacial cracks, then from an energy-minimization perspective, the expression for $Q_2(c)$ can be written as [41]

$$Q_2 = \frac{\partial Q_1}{\partial \Delta_x}\sqrt{2\gamma \frac{\partial A_1}{\partial \Delta_x}\Big/\frac{\partial^2 Q_1}{\partial \Delta_x^2}}, \tag{20}$$

where $A_1 = \pi c^2$ is the area of the stick zone, and Δ_x is the tangential displacement associated with Q_1, given by

$$\Delta_x = \frac{c^2}{(k+1)R_T}, \tag{21}$$

with R_T determined, based on the conclusion of Sec. 2.1, as

$$R_T = \frac{G_0^*}{fE_0^*}R = \frac{1}{f\alpha}R, \tag{22}$$

where α represents the ratio of the normal stiffness to the tangential stiffness, and is derived in the same form as that provided in Ref. [32], namely

$$\alpha\left(k, \nu_i, \frac{E_{01}}{E_{02}}\right) = \frac{E_0^*}{G_0^*} = \frac{\frac{1}{h_T(k,\nu_1)E_{01}} + \frac{1}{h_T(k,\nu_2)E_{02}}}{\frac{1-\nu_1^2}{h_N(k,\nu_1)E_{01}} + \frac{1-\nu_2^2}{h_N(k,\nu_2)E_{02}}}. \tag{23}$$

By combining Eqs. (17), (20), (21), (22), and the relationship $Q_1(c) = fP_1(c)$, we obtain

$$Q_2(c) = \sqrt{\frac{8\pi\gamma G_0^* c^{3+k}}{z_0^k (1+k)^2}}, \tag{24}$$

and therefore the final distribution of the tangential traction inside the stick zone can be determined using $q(r) =$

$fp(r,a) - q^*_{\mathrm{JKR}}(r,c)$. Furthermore, since the normal and tangential problems are decoupled, the normal load is simply given by $P = P_1(a)$, while the tangential load, based on the tangential traction distribution, can be determined as

$$Q = f\left[P_1(a) - P_1(c)\right] + Q_2(c), \tag{25}$$

and in dimensionless form as

$$\frac{Q}{fP} = 1 - \left(\frac{c}{a}\right)^{3+k} + 2\eta\sqrt{\frac{3+k}{\alpha}}\left(\frac{c}{a}\right)^{\frac{3+k}{2}}, \tag{26}$$

where the dimensionless parameter η is defined as

$$\eta = \sqrt{\frac{\pi\gamma R}{2f^2P}}. \tag{27}$$

In addition, based on the tangential traction distribution, the relative tangential rigid-body displacement between the two spheres, denoted by δ_T, can also be obtained from Eqs. (10), (21), and (22), and is given in dimensionless form by

$$\frac{\delta_T}{f\delta_z} = \alpha\left[1 - \left(\frac{c}{a}\right)^2\right] + 4\eta\sqrt{\frac{\alpha}{3+k}}\left(\frac{c}{a}\right)^{\frac{1-k}{2}}, \tag{28}$$

where δ_z denotes the normal relative rigid-body displacement, as given in Eq. (18).

It is worth noting that when $c/a = 1$, corresponding to full stick within the entire contact region, both the tangential force Q and the tangential displacement δ_T are non-zero. For any tangential load Q below its value at $c/a = 1$, the contact remains in full stick, and the relation between Q and δ_T is linear. In this full-stick regime, the relationship between Q and δ_T can be expressed as

$$\frac{Q}{fP} = \frac{3+k}{2\alpha}\frac{\delta_T}{f\delta_z}, \quad \text{for } \frac{Q}{fP} \leqslant 2\eta\sqrt{\frac{3+k}{\alpha}}. \tag{29}$$

Once Q exceeds the threshold given in Eq. (29), the stick zone shrinks and the contact enters the partial-slip regime, as described in Eqs. (26) and (28).

3 Constant frictional fracture energy

It is worth emphasizing that all the formulas in this paper are universal under the assumption of decoupled tangential and normal responses. However, in generating the results we assumed $E_{01} = E_{02} = E_0$ and $\nu_1 = \nu_2 = \nu$. Figure 2 shows the relationship between the dimensionless tangential force and the dimensionless tangential displacement for different values of η when $k = 0.5$ and $\nu = 0.5$. At the beginning of the tangential loading, the interface is in a state of full stick, as described by Eq. (29), which is represented by the black dash-dot line in the figure. When the critical condition given by Eq. (29) is reached, partial slip initiates, and the tangential force and displacement are then governed by Eqs. (26) and (28).

For $\eta = 0$, the response corresponds to the classical CM model, where the full-stick region vanishes and partial slip occurs immediately upon the onset of tangential loading. The tangential force increase monotonically with the tangential displacements, until the tangential force reaches the kinetic friction level.

For $\eta = 0.5$ and 0.8, after the onset of partial slip, the tangential force continues to increase with displacement and reaches a maximum value. In these cases, the maximum tangential force, denoted by $Q_{\max}$, and the corresponding the stick zone size, denoted by c_0, can be written as

$$\frac{Q_{\max}}{fP} = 1 + \frac{3+k}{\alpha}\eta^2, \tag{30}$$

$$\frac{c_0}{a} = \left[\eta\sqrt{\frac{3+k}{\alpha}}\right]^{\frac{2}{3+k}}. \tag{31}$$

These points are indicated by asterisks in Fig. 2. Beyond this point, the tangential force decreases with further displacement and is shown with dashed lines. Under force-controlled loading, this decreasing branch is unstable, and the interface will suddenly jump into the gross-slip regime, where the tangential force equals the kinetic friction.

For $\eta = 1.1$, once partial slip begins, Eqs. (26) and (28) predict that both the tangential force and displacement decrease. In this case, the response is unstable under either force-controlled or displacement-controlled loading, and the interface instantaneously transitions from full stick to gross slip. Therefore, no partial-slip regime exists for this value of η.

It can be shown that, in the tangential loading process illustrated in Fig. 2, Eq. (30) yields the maximum tangential force when the condition $\eta\sqrt{(3+k)/\alpha} \leqslant 1$ is satisfied. When $\eta\sqrt{(3+k)/\alpha} > 1$, the maximum tangential force is instead achieved exactly at the transition from full stick to gross slip (where no partial-slip regime exists). Therefore, the maximum static friction force can be written in a complete form as:

$$\frac{f_s}{f} = \frac{Q_{\max}}{fP} = \begin{cases} 1 + \frac{3+k}{\alpha}\eta^2, & \eta\sqrt{\frac{3+k}{\alpha}} \leqslant 1 \\ 2\eta\sqrt{\frac{3+k}{\alpha}}, & \eta\sqrt{\frac{3+k}{\alpha}} > 1 \end{cases}, \tag{32}$$

where $f_s = Q_{\max}/P$ is the static friction coefficient. It should be noted that the denominator of η contains P, and therefore the ratio f_s/f is pressure-dependent.

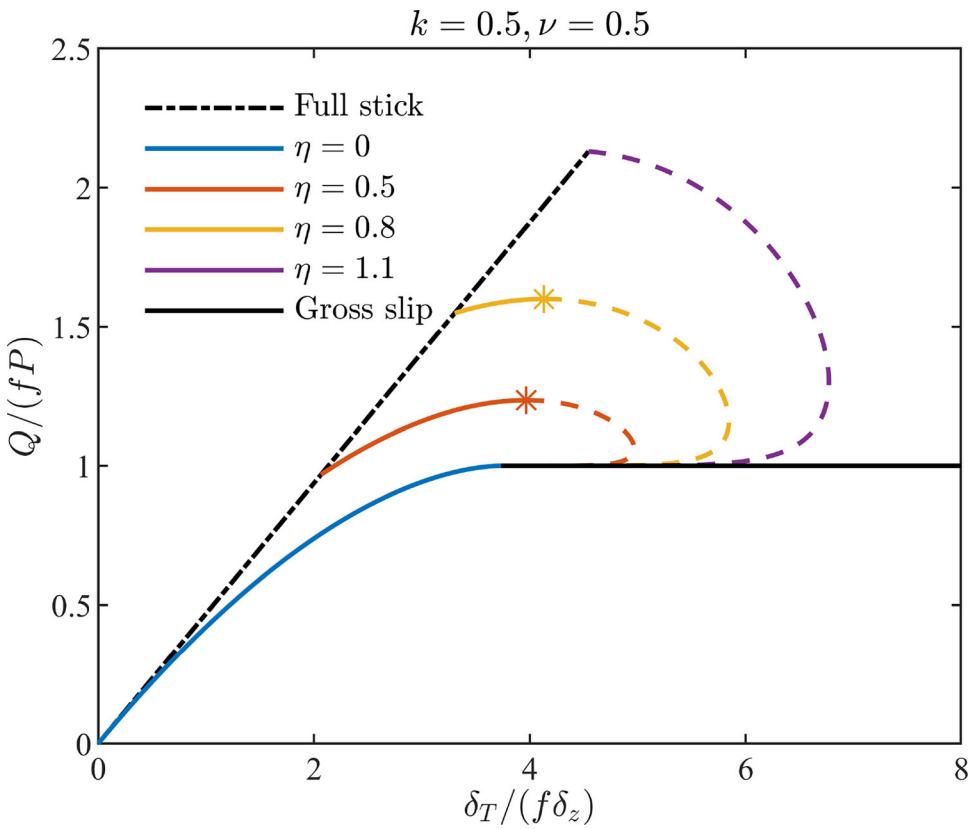

Fig. 2 Relationship between the tangential relative rigid-body displacement and the tangential force for different values of η with $k = 0.5$ and $\nu = 0.5$, and constant frictional fracture energy

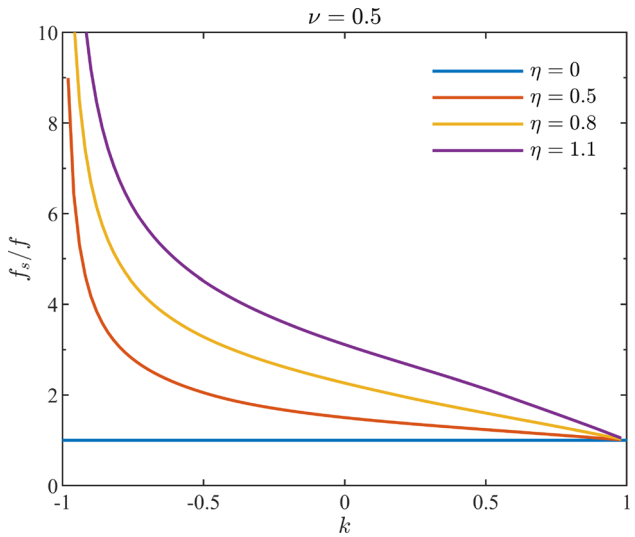

Fig. 3 Dependence of the static friction coefficient on the grading exponent k for different values of η, and constant frictional fracture energy

Figure 3 plots the ratio of the static to kinetic friction coefficients as a function of the material grading exponent k. It can be seen that the more common grading of softer surface and rigid substrates leads to a reduction of the difference between static and kinetic friction coefficient with respect to the homogeneous case. It is remarkable instead that the limit case of an infinitely rigid surface leads to infinite static friction.

Equation (32) indicates that, due to the dependence of the parameter η on the normal load, the ratio of static to kinetic friction coefficients is load-dependent. However, this formula does not explicitly include a direct dependence on the normal load. Therefore, in order to better describe this load dependence, we can rewrite the parameter η as

$$\eta = \psi\sqrt{\frac{P_{\text{ref}}}{P}}, \text{ where } \psi = \sqrt{\frac{\pi\gamma R^2}{2f^2E_0z_0^3}}, \tag{33}$$

with $P_{\text{ref}} = E_0z_0^3/R$. Figure 4 plots the relation between the static friction coefficient and the normal load. It is shown that static friction strongly decreases with normal load, while in the limit of zero load we would have in principle an infinite static friction.

4 Pressure-dependent frictional fracture energy

Since solid surfaces are generally rough, the actual contact between two solids occurs at fragmented patches, and the real contact area constitutes only a small fraction of the apparent contact area. Numerous previous studies have shown that,

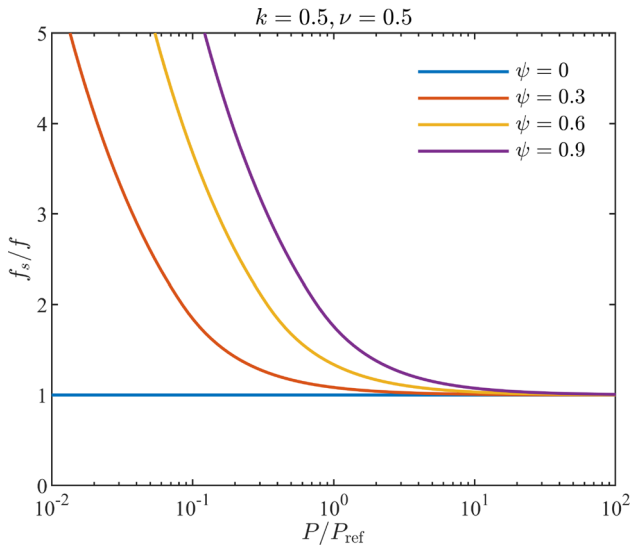

Fig. 4 Dependence of the static friction coefficient on the normal load for different values of ψ and $k = 0.5$, and constant frictional fracture energy

under relatively small loads, the real contact area is proportional to the applied normal load. Therefore, as suggested by Ciavarella in Ref. [11], it's more realistic to assume that the frictional fracture energy γ is proportional to the real contact area and, consequently, to the pressure due to the existence of surface roughness. We denote the frictional fracture energy at a reference pressure p_{ref} by γ_{ref}. The pressure-dependent frictional fracture energy γ_{pd} can then be expressed as

$$\gamma_{\text{pd}} = \frac{\gamma_{\text{ref}}}{p_{\text{ref}}} p_0 \left(1 - \frac{c^2}{a^2}\right)^{\frac{1+k}{2}}, \tag{34}$$

with

$$p_0 = \frac{(3+k)P}{2\pi a^2}. \tag{35}$$

Therefore, we can also rewrite η in a reduced form as

$$\eta_{\text{pd}} = \sqrt{\frac{\pi \gamma_{\text{pd}} R}{2 f^2 P}} = h_{\text{pd}} \psi_{\text{pd}} \left(\frac{P_{\text{ref}}}{P}\right)^{\frac{1}{3+k}} \left(1 - \frac{c^2}{a^2}\right)^{\frac{1+k}{4}}, \tag{36}$$

with

$$h_{\text{pd}}(k, \nu) = \sqrt{\frac{3+k}{4}} \left[\frac{4E_0^*}{E_0 (1+k)^2 (3+k)}\right]^{\frac{1}{3+k}}, \tag{37}$$

$$\psi_{\text{pd}} = \sqrt{\frac{\gamma_{\text{ref}} R}{f^2 z_0^2 p_{\text{ref}}}}, \tag{38}$$

and $P_{\text{ref}} = E_0 z_0^3 / R$ is a reference force.

By substituting Eq. (36) into Eqs. (26) and (28), the effect of the pressure-dependent frictional fracture energy is incorporated into the formulation. Eq. (26) can be rewritten as

$$\frac{Q}{fP} = 1 - \left(\frac{c}{a}\right)^{3+k} + 2 h_{\text{pd}} \psi_{\text{pd}} \sqrt{\frac{3+k}{\alpha}} \left(\frac{P_{\text{ref}}}{P}\right)^{\frac{1}{3+k}} \left(1 - \frac{c^2}{a^2}\right)^{\frac{1+k}{4}} \left(\frac{c}{a}\right)^{\frac{3+k}{2}}. \tag{39}$$

and Eq. (28) can be rewritten as

$$\frac{\delta_T}{f \delta_z} = \alpha \left[1 - \left(\frac{c}{a}\right)^2\right] + 4 h_{\text{pd}} \psi_{\text{pd}} \sqrt{\frac{\alpha}{3+k}} \left(\frac{P_{\text{ref}}}{P}\right)^{\frac{1}{3+k}} \left(1 - \frac{c^2}{a^2}\right)^{\frac{1+k}{4}} \left(\frac{c}{a}\right)^{\frac{1-k}{2}}. \tag{40}$$

After incorporating the pressure-dependent frictional fracture energy, the expressions for the tangential force and tangential displacement become considerably more complex, making it difficult to obtain a simple closed-form expression for the static friction coefficient. However, by applying standard mathematical procedures, namely, by differentiating Eq. (39) with respect to c/a, the stick zone radius corresponding to the maximum static friction, c_0, can be determined as the solution of the following equation:

$$\left(\frac{c_0}{a}\right)^{\frac{3+k}{2}} = 2 h_{\text{pd}} \psi_{\text{pd}} \sqrt{\frac{3+k}{\alpha}} \left(\frac{P_{\text{ref}}}{P}\right)^{\frac{1}{3+k}} \left[\frac{1}{2} - \frac{(2+k)}{(3+k)} \left(\frac{c_0}{a}\right)^2\right] \left[1 - \left(\frac{c_0}{a}\right)^2\right]^{\frac{k-3}{4}}. \tag{41}$$

By substituting c_0 into Eqs. (39) and (40), the maximum friction and the corresponding tangential displacement can be determined.

Fig. 5, 6 and 7 show the corresponding results of Fig. 2, 3 and 4, but with pressure-dependent friction energy. The trends are very similar, except that full stick is now removed as possibility.

To compare the pressure-dependent fracture energy (PDFE) scenario with the constant fracture energy (CFE) one, Fig. 8 shows the static friction coefficient as a function of normal load for the CFE case and for the PDFE case with various grading exponents k. The values of ψ and ψ_{pd} are both taken as 0.3; these parameters only produce a horizontal shift in the log-log plots of Fig. 8. The figure indicates that the difference between the two theories is negligible for loads larger than the reference load, and becomes significant only at low loads, where the static friction coefficient diverges more slowly under the PDFE assumption. In the low-load regime, Eq. (32)

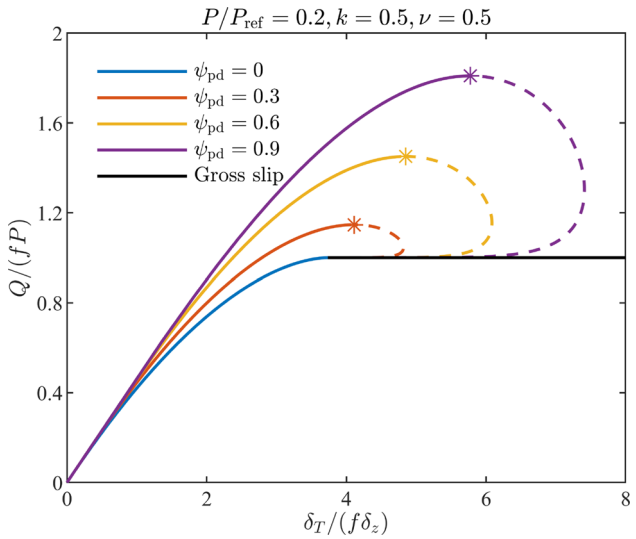

Fig. 5 Tangential force $Q/(fP)$ as a function of $\delta_T/(f\delta_z)$ for different $\psi_{\rm pd}$ and $P/P_{\rm ref} = 0.2$ and $k = 0.5$, and pressure-dependent frictional fracture energy

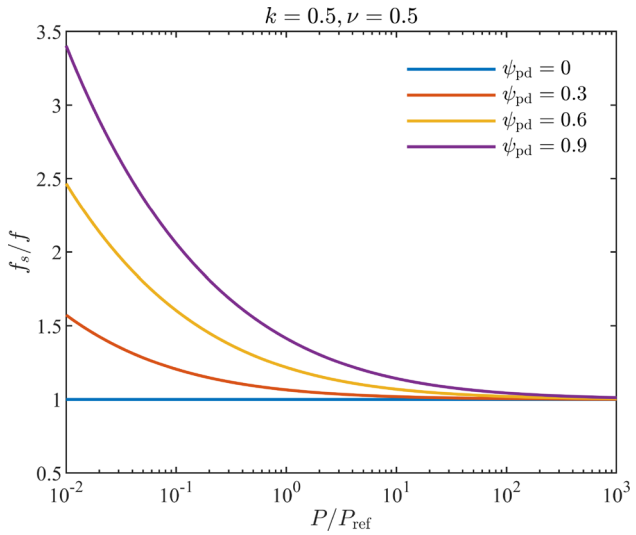

Fig. 6 Dependence of the static friction coefficient on the normal load for different values of $\psi_{\rm pd}$ and $k = 0.5$, and pressure-dependent frictional fracture energy

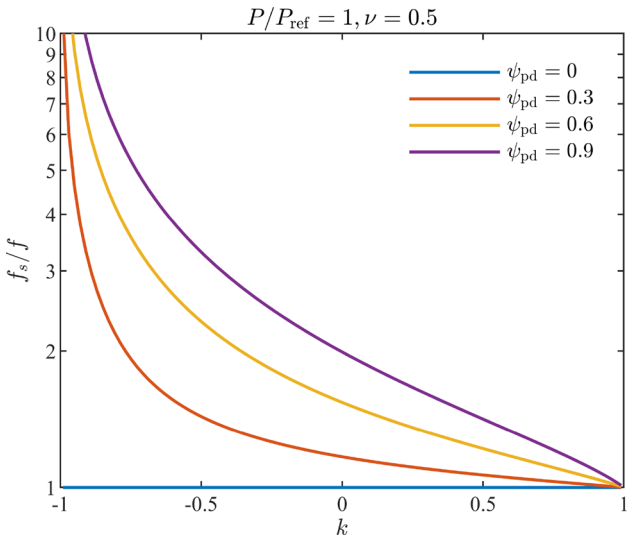

Fig. 7 Dependence of the static friction coefficient on the grading exponent k for different values of $\psi_{\rm pd}$ and $P/P_{\rm ref} = 1$, and pressure-dependent frictional fracture energy

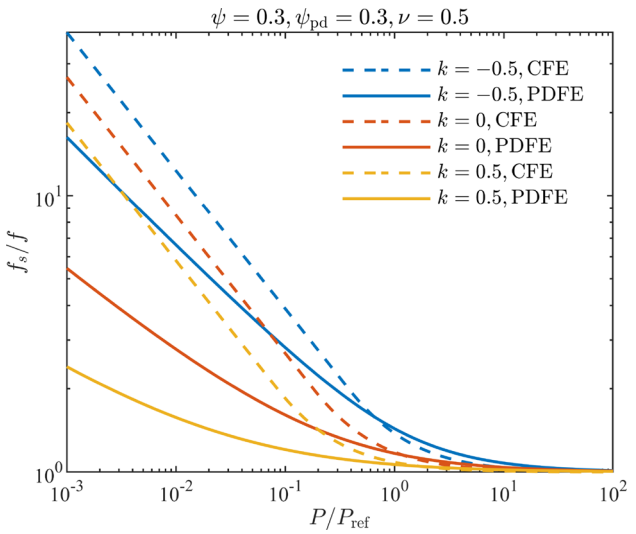

Fig. 8 Static friction coefficient as a function of normal load for the constant fracture energy (CFE) case and the pressure-dependent fracture energy (PDFE) case with various grading exponents k and $\psi = \psi_{\rm pd} = 0.3$

shows that in the CFE case $f_s \sim P^{-1/2}$ for any k, whereas under the PDFE assumption the rate of increase of f_s with decreasing P is evidently diminished.

Figure 9 plots instead the radius of the stick zone at the maximum tangential force as a function of normal load for the CFE case and the PDFE case with various grading exponents k. Notice that the instability at very low normal load occurs already with the entire area in stick for the case of constant friction energy, while this never occurs for pressure-dependent friction energy.

5 Conclusions

In view of the fundamental question of how coefficient of friction results from the fracture mechanics of "Griffith friction" for a basic sphere-sphere geometry, we have studied the role of gradient in the material properties of contacting bodies. The difference between static and kinetic friction depends on where the transition from stick to slip occurs as an elastic instability. The theory is fully analytical and shows that static friction coefficient: (i) is increased with harder surface; (ii) is increased for small normal loads and tends to infinity in

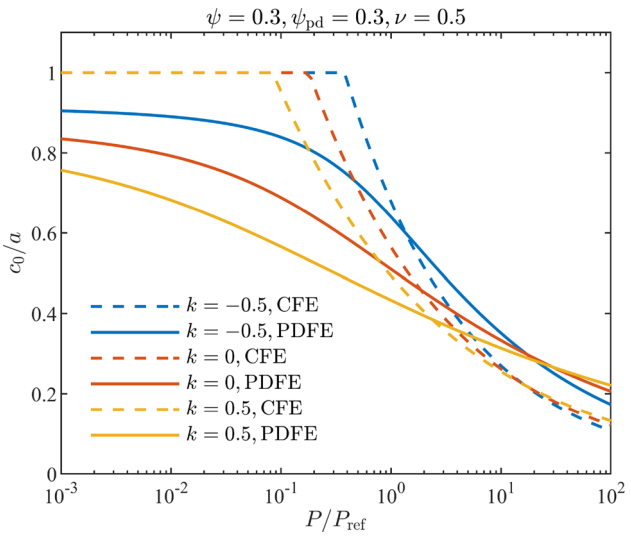

Fig. 9 Radius of the stick zone at the maximum tangential force as a function of normal load for the constant fracture energy (CFE) case and the pressure-dependent fracture energy (PDFE) case with various grading exponents k and $\psi = \psi_{pd} = 0.3$

the limit of zero load, whereas it tends to the kinetic friction coefficient at large normal loads. There are quantitative differences in the conclusions if we assume a constant frictional fracture energy or a pressure-dependent frictional fracture energy at the interface.

Finally, we emphasize that throughout the present study, the contacting solids are assumed to possess the same grading exponent. In fact, contact problems involving different grading exponents have already been investigated in the literature [42]. Extending the present framework to account for dissimilar grading exponents would represent a natural and meaningful direction for further refinement and generalization of the model.

Acknowledgements MC acknowledges support from the Italian Ministry of Education, University and Research (MIUR) under the program Departments of Excellence (L.232/2016) and PRIN 2022 (Project ID: Prot.2022Y78C3K, CUP: D53C24004340006). GFW and SWC acknowledge support from the National Natural Science Foundation of China (Grant No. 12372100). SWC also acknowledges financial support from the China Scholarship Council.

Author Contributions SWC: Formal analysis, Methodology, Software, Validation, Visualization, Writing - original draft, Writing - review & editing. GFW: supervision, funding acquisition. MC: Conceptualization, Investigation, Methodology, Writing - original draft, Writing - review & editing.

Funding Open access funding provided by Politecnico di Bari within the CRUI-CARE Agreement.

Data Availability No datasets were generated or analyzed during the current study.

Declarations

Conflict of interest The authors declare no conflict of interest.

References

1. Rabinowicz, E.: The nature of the static and kinetic coefficients of friction. J. Appl. Phys. **22**(11), 1373–1379 (1951)
2. Rabinowicz, E.: Friction and wear of materials, 2nd edn,: New York. John Wiley, NY (1995)
3. Poliakov, A.N.B., Dmowska, R., Rice, J.R.: Dynamic shear rupture interactions with fault bends and off-axis secondary faulting. J. Geophys. Res. **107**(B11), 2295 (2002)
4. Rice, J.R.: Low-stress faulting: strong but brittle faults with local stress concentrations. Eos Trans. AGU 77, Fall Meet. Suppl., F471, (1996)
5. Johnson, K.L., Kendall, K., Roberts, A.D.: Surface energy and contact of elastic solids. Proc. R. Soc. Lond. A Math. Phys. Sci. **324**(1558), 301–313 (1971)
6. Ida, Y.: Cohesive force across the tip of a longitudinal-shear crack and griffith's specific surface energy. J. Geophys. Res. **77**(20), 3796–3805 (1972)
7. Maugis, D., Barquins, M.: Fracture mechanics and the adherence of viscoelastic bodies. J. Phys. D Appl. Phys. **11**(14), 1989 (1978)
8. Palmer, A.C., Rice, J.R.: The growth of slip surfaces in the progressive failure of over-consolidated clay. Proc. R. Soc. Lond. A Math. Phys. Sci. **332**(1591), 527–548 (1973)
9. Savkoor, A.R., Briggs, G.A.D.: The effect of tangential force on the contact of elastic solids in adhesion. Proc. R. Soc. Lond. A Math. Phys. Sci. **356**(1684), 103–114 (1977)
10. Argatov, I.I., Lyashenko, I.A., Popov, V.L.: Adhesive sliding with a nominal point contact: postpredictive analysis. Int. J. Eng. Sci. **200**, 104055 (2024)
11. Ciavarella, M.: Transition from stick to slip in hertzian contact with "griffith" friction: the cattaneo-mindlin problem revisited. J. Mech. Phys. Solids **84**, 313–324 (2015)
12. Cattaneo, C.: Sul Contatto di due Corpore Elastici: Distribuzione degli sforzi. Rendiconti Dell'Acad. Nazionale Dei Lincei, 27: p. 342-348, 434-436, 474-478 (1938)
13. Mindlin, R.D.: Compliance of elastic bodies in contact. J. Appl. Mech. **16**(3), 259–268 (1949)
14. Peng, L., et al.: Decrease of Static Friction Coefficient with Interface Growth from Single to Multiasperity Contact. Phys. Rev. Lett. **134**(17), 176202 (2025)
15. Ciavarella, M.: On the Dependence of Static Friction Coefficient on Normal Load. Tribol. Lett. **73**(4), 130 (2025)

16. Bhushan, B., Gupta, B.K.: Handbook of tribology: materials, coatings, and surface treatments. McGraw-Hill, New York (1991)
17. Roos, J.R., et al.: The development of composite plating for advanced materials. JOM **42**(11), 60–63 (1990)
18. Erdogan, F.: Fracture mechanics of functionally graded materials. Compos. Eng. **5**(7), 753–770 (1995)
19. Jha, D.K., Kant, T., Singh, R.K.: A critical review of recent research on functionally graded plates. Compos. Struct. **96**, 833–849 (2013)
20. Birman, V., Keil, T., Hosder, S.: Functionally graded materials in engineering, in Structural interfaces and attachments in biology, pp. 19–41. Springer, New York (2013)
21. Udupa, G., Rao, S.S., Gangadharan, K.V.: Functionally Graded Composite Materials: An Overview. Proc. Mater. Sci. **5**, 1291–1299 (2014)
22. Selvadurai, A.P.S.: The Analytical Method in Geomechanics. Appl. Mech. Rev. **60**(3), 87–106 (2007)
23. Borowicka, H.: Die Druckausbreitung im Halbraum bei linear zunehmendem Elastizitätsmodul. Ingenieur-Archiv **14**(2), 75–82 (1943)
24. Taylor, D.W.: Fundamentals of soil mechanics. Wiley, New York (1948)
25. Gibson, R.E.: Some Results Concerning Displacements and Stresses in a Non-Homogeneous Elastic Half-space. Géotechnique **17**(1), 58–67 (1967)
26. Booker, J.R., Balaam, N.P., Davis, E.H.: The behaviour of an elastic non-homogeneous half-space. Part I-line and point loads. Int. J. Numer. Anal. Meth. Geomech. **9**(4), 353–367 (1985)
27. Booker, J.R., Balaam, N.P., Davis, E.H.: The behaviour of an elastic non-homogeneous half-space. Part II-circular and strip footings. Int. J. Numer. Anal. Meth. Geomech. **9**(4), 369–381 (1985)
28. Giannakopoulos, A.E., Suresh, S.: Indentation of solids with gradients in elastic properties: Part I. Point force. Int. J. Solids Struct. **34**(19), 2357–2392 (1997)
29. Giannakopoulos, A.E., Suresh, S.: Indentation of solids with gradients in elastic properties: Part II. axisymmetric indentors. Int. J. Solids Struct. **34**(19), 2393–2428 (1997)
30. Jitcharoen, J., et al.: Hertzian-Crack Suppression in Ceramics with Elastic-Modulus-Graded Surfaces. J. Am. Ceram. Soc. **81**(9), 2301–2308 (1998)
31. Suresh, S., et al.: Engineering the resistance to sliding-contact damage through controlled gradients in elastic properties at contact surfaces. Acta Mater. **47**(14), 3915–3926 (1999)
32. Popov, V.L., M. Hess, Willert, E.: Contact Problems of Functionally Graded Materials, in Handbook of Contact Mechanics: Exact Solutions of Axisymmetric Contact Problems, V.L. Popov, M. Hess, and E. Willert, Editors. Springer Berlin Heidelberg: Berlin, Heidelberg. p. 251-293 (2019)
33. Mossakovskii, V.I.: Compression of elastic bodies under conditions of adhesion (Axisymmetric case). J. Appl. Math. Mech. **27**(3), 630–643 (1963)
34. Jager, J.: Axisymmetrical bodies of equal material in contact under torsion or shift. Arch. Appl. Mech. **65**(7), 478–487 (1995)
35. Greenwood, J.A.: Contact between an axisymmetric indenter and a viscoelastic half-space. Int. J. Mech. Sci. **52**(6), 829–835 (2010)
36. Hess, M., Popov, V.L.: Method of dimensionality reduction in contact mechanics and friction: a user's handbook. II. Power-law graded materials. Facta Universitatis, Series: Mechanical Engineering **14**(3), 251–268 (2016)
37. Hess, M., Li, Q.: Tangential contacts of three-dimensional power-law graded elastic solids: A general theory and application to partial slip. Mech. Adv. Mater. Struct. **31**(23), 5885–5905 (2024)
38. Chai, Y.S., Argatov, I.I.: Local tangential contact of elastically similar, transversely isotropic elastic bodies. Meccanica **53**(11), 3137–3143 (2018)
39. Svetlizky, I., Fineberg, J.: Classical shear cracks drive the onset of dry frictional motion. Nature **509**(7499), 205–208 (2014)
40. Anderson, T.L.: Fracture Mechanics: Fundamentals and Applications, (2017). CRC Press
41. Ciavarella, M.: An approximate JKR solution for a general contact, including rough contacts. J. Mech. Phys. Solids **114**, 209–218 (2018)
42. Antipov, Y.A., Mkhitaryan, S.M.: Axisymmetric contact of two different power-law graded elastic bodies and an integral equation with two Weber-Schafheitlin kernels. Q. J. Mech. Appl. Math. **75**(4), 393–420 (2022)